



This is a repository copy of *Aldehyde-functional diblock copolymer nano-objects via RAFT aqueous dispersion polymerization*.

White Rose Research Online URL for this paper:

<https://eprints.whiterose.ac.uk/183028/>

Version: Accepted Version

Article:

Brotherton, E.E., Smallridge, M.J. and Armes, S.P. orcid.org/0000-0002-8289-6351 (2021) Aldehyde-functional diblock copolymer nano-objects via RAFT aqueous dispersion polymerization. *Biomacromolecules*, 22 (12). pp. 5382-5389. ISSN 1525-7797

<https://doi.org/10.1021/acs.biomac.1c01327>

This document is the Accepted Manuscript version of a Published Work that appeared in final form in *Biomacromolecules*, copyright © American Chemical Society after peer review and technical editing by the publisher. To access the final edited and published work see <https://doi.org/10.1021/acs.biomac.1c01327>.

Reuse

Items deposited in White Rose Research Online are protected by copyright, with all rights reserved unless indicated otherwise. They may be downloaded and/or printed for private study, or other acts as permitted by national copyright laws. The publisher or other rights holders may allow further reproduction and re-use of the full text version. This is indicated by the licence information on the White Rose Research Online record for the item.

Takedown

If you consider content in White Rose Research Online to be in breach of UK law, please notify us by emailing eprints@whiterose.ac.uk including the URL of the record and the reason for the withdrawal request.



eprints@whiterose.ac.uk
<https://eprints.whiterose.ac.uk/>

Aldehyde-functional diblock copolymer nano-objects via RAFT aqueous dispersion polymerization

E. E. Brotherton^a, M. J. Smallridge^b and S. P. Armes^{a,*}

a. Dainton Building, Department of Chemistry, The University of Sheffield,
Brook Hill, Sheffield, South Yorkshire, S3 7HF, UK.

b. GEO Specialty Chemicals, Hythe, Southampton, Hampshire SO45 3ZG, UK.

Abstract. We report the rational design of aldehyde-functional sterically-stabilized diblock copolymer nano-objects in aqueous solution *via* polymerization-induced self-assembly (PISA). More specifically, the RAFT aqueous dispersion polymerization of 2-hydroxypropyl methacrylate (HPMA) is conducted using a water-soluble precursor block in which every methacrylic repeat unit contains a pendent oligo(ethylene glycol) side-chain capped with a *cis*-diol unit. Systematic variation of the reaction conditions enables the construction of a pseudo-phase diagram, which ensures the reproducible targeting of pure spheres, worms or vesicles. Selective oxidation of the pendent *cis*-diol groups using aqueous sodium periodate under mild conditions introduces geminal diols (i.e., the hydrated form of an aldehyde obtained in the presence of water) into the steric stabilizer chains without loss of colloidal stability. In the case of diblock copolymer vesicles, such derivatization leads to the formation of a worm population, i.e. partial loss of the original morphology. However, this problem can be circumvented by crosslinking the membrane-forming block prior to periodate oxidation. Moreover, such covalently-stabilized aldehyde-functionalized vesicles can be subsequently reacted with either glycine or histidine in aqueous solution, followed by reduction amination to prevent hydrolysis of the labile imine bond. Zeta potential measurements confirm that this derivatization significantly affects the electrophoretic behavior of these vesicles. Similarly, the membrane-crosslinked aldehyde-functionalized vesicles can be reacted with a model globular protein, bovine serum albumin (BSA), to produce 'stealthy' protein-decorated vesicles.

* To whom correspondence should be addressed (s.p.arnes@shef.ac.uk)

Introduction

Block copolymer self-assembly in solution has been studied for more than fifty years.¹⁻³ Traditionally, this has been achieved by post-polymerization processing in dilute solution,^{4,5} but over the past decade polymerization-induced self-assembly (PISA) has emerged as a versatile platform technology for the rational synthesis of various block copolymer nano-objects in the form of concentrated colloidal dispersions.⁶⁻⁸ PISA involves growing an insoluble block from a soluble precursor block in a suitable selective solvent to produce sterically-stabilized nanoparticles, with the three most common copolymer morphologies being spheres, worms and vesicles.⁹⁻¹¹ At intermediate conversions, the unreacted monomer effectively acts as a processing aid or co-solvent for the growing insoluble block.⁶ This approach works well in various solvents, including water. In the case of aqueous PISA, there are two possible formulations. Typically, the vinyl monomer used to grow the second block is water-immiscible, which leads to an aqueous emulsion polymerization. On the other hand, if the vinyl monomer is water-miscible then this corresponds to an aqueous dispersion polymerization. PISA can be performed using various (pseudo-)living techniques but the most commonly reported technique in the literature is undoubtedly reversible addition-fragmentation chain transfer (RAFT) polymerization.¹² This is no doubt because RAFT polymerization offers excellent tolerance of monomer functionality, can be conducted under a wide range of conditions and offers the possibility of introducing desirable end-groups by selecting an appropriate RAFT agent.^{13,14}

Aqueous PISA has been used to prepare many examples of functional block copolymer nano-objects. For example, disulfide bonds have been incorporated to prepare thiol-functionalized block copolymer worms and vesicles^{15,16} while glycidyl methacrylate has been used as a comonomer to introduce epoxy groups into the water-insoluble structure-directing block.¹⁷⁻²¹ Similarly, diacetone acrylamide (DAAM) confers ketone functionality, which has been exploited for both metal complexation²² and post-polymerization cross-linking.²³ Brendel and co-workers have reported the design of oxidation-sensitive nano-objects based on a thiamorpholine monomer.²⁴ Rieger and co-workers have

demonstrated that using a bisurea-based RAFT agent leads to extensive hydrogen bonding within the core-forming block that strongly favors the formation of the worm morphology.²⁵ Armes and co-workers have shown that using either carboxylic acid-based or tertiary amine-based RAFT agents enables the design of pH-responsive diblock copolymer nano-objects that can switch morphology simply by introducing a single ionic charge at the end of each steric stabilizer chain.^{26,27} If poly(glycerol monomethacrylate) (PGMA) is used as a steric stabilizer block, its pendent *cis*-diol groups can be used to ensure selective adsorption of the resulting nanoparticles onto an appropriately patterned 2D surface.²⁸ Alternatively, binding of water-soluble phenylboronic acid derivatives to diblock copolymer vesicles in alkaline solution can induce a change in copolymer morphology to produce either worms or spheres, thereby releasing any cargo encapsulated within the vesicle lumen.^{29,30} Finally, the highly hydroxylated nature of the PGMA block appears to be essential for inducing stasis in human stem cell colonies immersed within PGMA-based worm gels.³¹

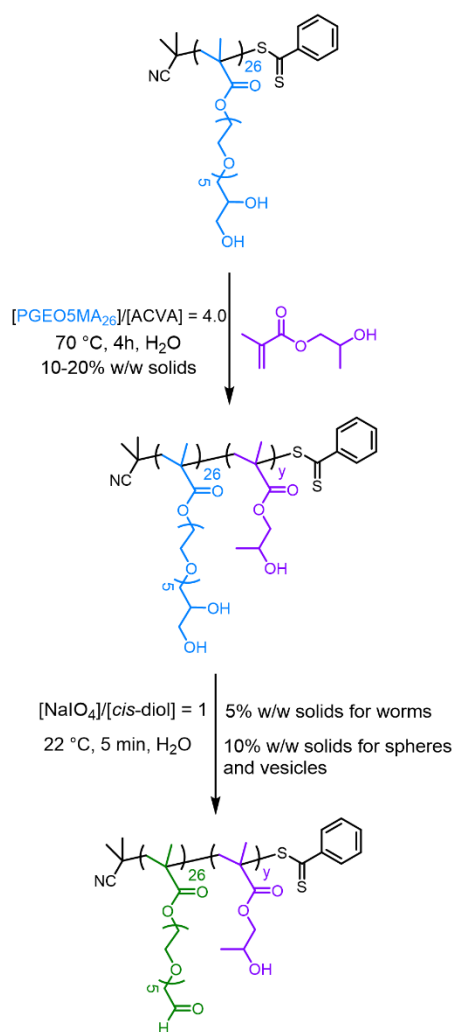
However, as far as we are aware, there have been no reports of aldehyde-functional block copolymer nano-objects prepared by aqueous PISA. This is perhaps surprising because aldehyde chemistry offers many possibilities for derivatization. In particular, conjugation to amine-functional (macro)molecules via Schiff base chemistry³² can be conducted in aqueous solution under mild conditions, which is expected to offer potential biomedical applications.^{33–58} Recently, we reported the synthesis of a new methacrylic monomer (GEO5MA; see Scheme S1) that resembles both glycerol monomethacrylate (GMA) and oligo(ethylene glycol) methacrylate (OEGMA).⁵⁹ Selective oxidation of the pendent *cis*-diol groups in GEO5MA (or its corresponding PGEO5MA homopolymer) using aqueous sodium periodate introduces a geminal diol group, which is simply the hydrated form of an aldehyde group. In the present study, we combine this chemistry with the RAFT aqueous dispersion polymerization of 2-hydroxypropyl methacrylate (HPMA) for the rational design of aldehyde-functional diblock copolymer spheres, worms and vesicles. We also conduct several model reactions on aqueous dispersions of these nano-objects under mild conditions using either amino acids or a common globular protein.

Results and Discussion

A PGEO5MA₂₆ homopolymer was synthesized *via* RAFT solution polymerization in ethanol. DMF GPC confirmed that this precursor had an M_n of 14.3 kg mol⁻¹ and a relatively narrow molecular weight distribution ($\mathcal{D} = 1.18$). This PGEO5MA₂₆ was then chain-extended *via* RAFT aqueous dispersion polymerization of 2-hydroxypropyl methacrylate (HPMA) (Scheme 1). The copolymer concentration and the PHPMA target degree of polymerization (DP) were systematically varied to afford a series of nanoparticles exhibiting various copolymer morphologies (Figure 1). Transmission electron microscopy (TEM) and dynamic light scattering (DLS) were employed to characterize these nanoparticles. For example, targeting PGEO5MA₂₆-PHPMA₁₇₀ at 10% w/w solids produced spherical nanoparticles as judged by TEM (Figure 1a) with a z-average diameter of 31 nm (DLS PDI = 0.02). On the other hand, PGEO5MA₂₆-PHPMA₂₄₀ nanoparticles prepared at 12.5% w/w solids exhibited a highly anisotropic worm-like morphology (Figure 1b) with a sphere-equivalent DLS diameter of 504 nm (PDI = 0.38). Targeting PGEO5MA₂₆-PHPMA₃₂₀ at 15% w/w solids produced a pure vesicular morphology (Figure 1c), with a DLS diameter of 397 nm (PDI = 0.19). Consequently, a PGEO5MA₂₆-PHPMA_y pseudo-phase diagram was constructed (Figure 1), with multilamellar vesicles (MLV; Figure 1d) with a DLS diameter of 515 nm (PDI = 0.23) being obtained when targeting PGEO5MA₂₆-PHPMA₃₂₀ at 20% w/w solids.

DMF GPC analysis showed that all diblock copolymers exhibited relatively low dispersities ($\mathcal{D} \leq 1.36$, Figure S1). However, high molecular weight shoulders can be observed in each case, which have been previously attributed to dimethacrylate impurities in the HPMA monomer (~0.20-0.35%).⁶⁰⁻⁶²

From the constructed phase diagram, three examples of PGEO5MA₂₆-PHPMA_y ($y = 170, 250$ and 350) nanoparticles were synthesized at 10% w/w solids. ¹H NMR spectroscopy studies indicated that the HPMA conversion was greater than 99% in each case. TEM analysis indicated a spherical morphology for PGEO5MA₂₆-PHPMA₁₇₀ nanoparticles (Figure S2a), a worm-like morphology for PGEO5MA₂₆-PHPMA₂₅₀ (Figure S3a) and a vesicular morphology for PGEO5MA₂₆-PHPMA₃₅₀ (Figure



Scheme 1. Two-step synthesis of a series of aldehyde-functionalized PAGE05MA₂₆-PHPMA_y diblock copolymer nano-objects starting from PGE05MA₂₆ homopolymer. First, this water-soluble precursor is chain-extended *via* RAFT aqueous dispersion polymerization of HPMA. The second step involves selective oxidation of the PGE05MA₂₆ block using aqueous sodium periodate at 22 °C.

S4a). Oxidation of the PGE05MA₂₆ block to produce an aldehyde-functional PAGE05MA₂₆ block was conducted using sodium periodate in aqueous solution using a recently reported protocol.⁵⁹ A NaIO₄/cis-diol molar ratio of unity was selected to target oxidation of all of the pendent *cis*-diol groups within the PGE05MA₂₆ block and the copolymer concentration was 5-10% w/w solids, which ensured efficient stirring. The extent of oxidation was determined to be more than 99% in each case by ¹H NMR spectroscopy as determined by the appearance of two new signals at 6.09 and 9.71 ppm corresponding to the geminal diol and aldehyde, respectively. For PGE05MA₂₆-PHPMA₁₇₀ spheres, DMF GPC analysis indicated that periodate oxidation had a significant effect on the copolymer molecular weight distribution: the PGE05MA₂₆-PHPMA₁₇₀ precursor had an M_n of 50.7 kg mol⁻¹ and a

\mathcal{D} of 1.21, whereas the PGE05MA₂₆-PHPMA₁₇₀ product had an M_n of 66.0 kg mol⁻¹ and a \mathcal{D} of 1.74 (Figure S5a). This was attributed to crosslinking between the aldehyde-functional group and the hydroxyl group on the HPMA units occurring at intermediate conversions. Perhaps surprisingly, periodate oxidation of the PGE05MA₂₆-PHPMA₂₅₀ worms led to a rather modest change in the copolymer molecular weight distribution ($M_n = 71.4$ kg mol⁻¹ and $\mathcal{D} = 1.30$ for the precursor vs. $M_n = 71.8$ kg mol⁻¹ and $\mathcal{D} = 1.37$ for the product (Figure S5b). This difference may be related to the lower copolymer concentration at which the worm oxidation reaction was conducted (5% w/w vs. 10% w/w). In both cases, TEM studies indicated that such oxidation did not affect the original copolymer

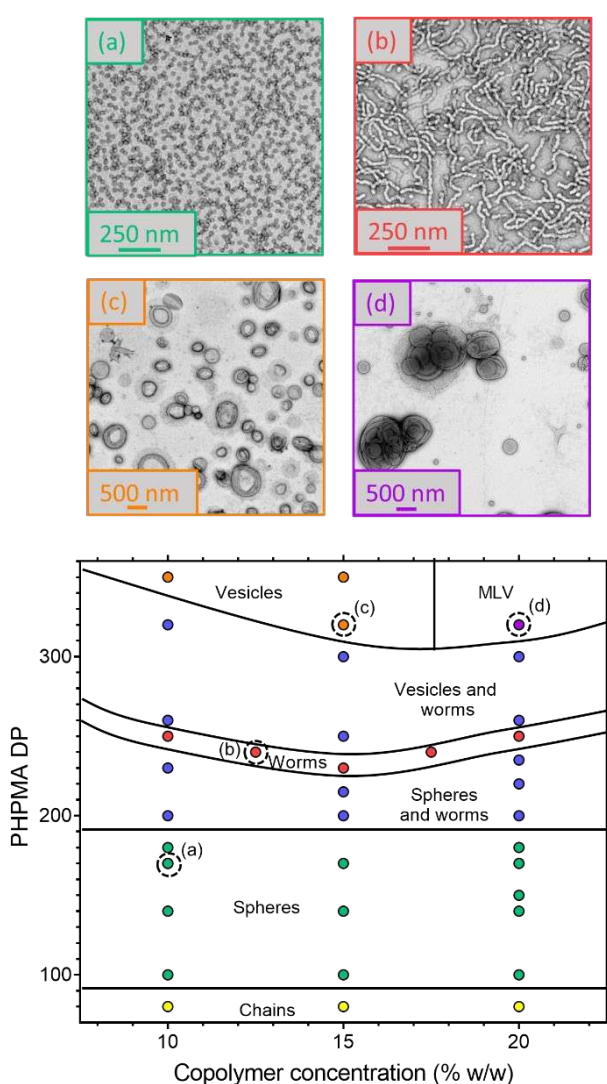


Figure 1. TEM images of (a) PGE05MA₂₆-PHPMA₁₇₀ spherical nanoparticles, (b) PGE05MA₂₆-PHPMA₂₄₀ anisotropic worms, (c) PGE05MA₂₆-PHPMA₃₂₀ vesicles, (d) PGE05MA₂₆-PHPMA₃₂₀ multilamellar vesicles (MLV), and (e) a PGE05MA₂₆-HPMA_y diblock copolymer phase diagram showing pure sphere, worm and vesicles morphologies could all be obtained.

morphology (Figures S2b and S3b). These observations were supported by DLS analysis. For example, PGEO5MA₂₆-PHPMA₁₇₀ spheres had a DLS diameter of 31 nm (PDI = 0.02), whereas the PAGEO5MA₂₆-PHPMA₁₇₀ spheres had a DLS diameter of 32 nm (PDI = 0.08). The DLS data for the PGEO5MA₂₆-PHPMA₂₅₀ and PAGEO5MA₂₆-PHPMA₂₅₀ worms showed large apparent particle diameters and high PDIs (409 nm (PDI = 0.44) and 242 nm (PDI = 0.26), respectively). However, as DLS measurements are based on a spherical model, these values do not correspond to either the worm length or width.

In contrast, DLS analysis suggested a modest reduction in the z-average vesicle diameter for the periodate-treated PGEO5MA₂₆-PHPMA₃₅₀ vesicles (231 nm diameter (PDI = 0.04) vs. 219 nm diameter (PDI = 0.09) while GPC studies indicated a significantly broader molecular weight distribution ($\bar{M}_w = 1.41$ vs. $\bar{M}_w = 2.09$ for PGEO5MA₂₆-PHPMA₃₅₀ and PAGEO5MA₂₆-PHPMA₃₅₀, respectively). More importantly, TEM studies revealed a minor worm population in addition to the oxidized vesicles (Figure S4b). These subtle differences in the copolymer molecular weight distribution and morphology observed after periodate treatment are not currently understood and further studies are clearly warranted.

To prevent the partial loss of the original vesicular morphology, 20 units of ethylene glycol dimethacrylate (EGDMA) crosslinker were added as a third block to crosslink the membrane-forming chains prior to periodate oxidation (Scheme S2).⁶³ The resulting covalently-stabilized vesicles (see TEM image shown in Figure 2a) had a slightly smaller z-average diameter (214 nm, PDI = 0.11) than the original linear vesicles (231 nm, PDI = 0.04). To confirm successful crosslinking, further DLS studies were conducted in ethanol, which is a good solvent for both blocks. Addition of ethanol to the linear vesicles led to a derived count rate (or scattered light intensity) that was two orders of magnitude lower than that observed in water (Table S1). In contrast, the derived count rate was reduced by only a factor of two for the crosslinked vesicles dispersed in ethanol, indicating successful crosslinking of the membrane-forming chains. The crosslinked vesicles were treated with periodate in aqueous solution. Unlike the linear vesicles, there was no TEM evidence for a worm population in this case

(Figure 2b). Hence covalent stabilization is sufficient to prevent degradation of the original vesicle morphology during oxidation of the PGEO5MA stabilizer chains.

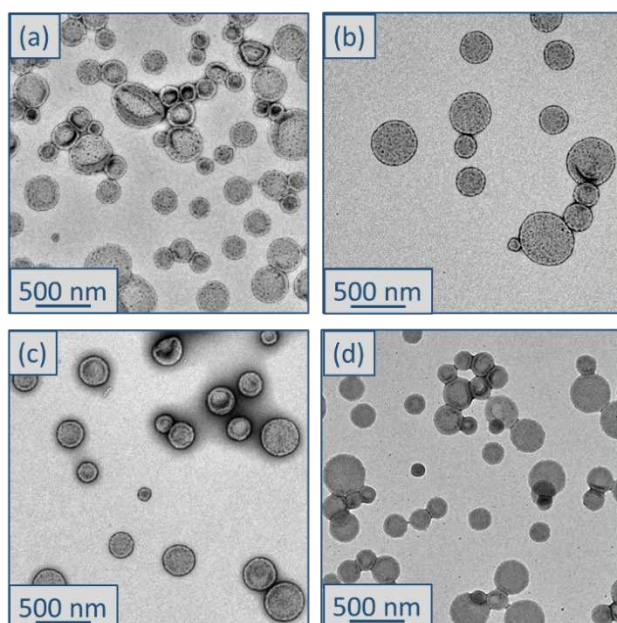


Figure 2. Transmission electron microscopy images recorded for (a) PGEO5MA₂₆-PHPMA₃₅₀-PEGDMA₂₀ vesicles, (b) PAGEO5MA₂₆-PHPMA₃₅₀-PEGDMA₂₀ vesicles, (c) PGlyGEO5MA₂₆-PHPMA₃₅₀-PEGDMA₂₀ vesicles and (d) PHisGEO5MA₂₆-PHPMA₃₅₀-PEGDMA₂₀ vesicles.

PAGEO5MA₂₆-PHPMA₁₇₀ spheres, PAGEO5MA₂₆-PHPMA₂₅₀ worms and PAGEO5MA₂₆-PHPMA₃₅₀-PEGDMA₂₀ vesicles were purified by dialysis against water and then reacted with either glycine or histidine *via* reductive amination (Scheme S3). An amino acid/aldehyde molar ratio of unity was used for the initial Schiff base reaction, with a 2.45 excess of NaCNBH₃ being employed as the reducing agent. ¹H NMR spectroscopy studies confirmed the mean degree of amino acid functionalization to be greater than 99% in both cases (Figure S6). Given the zwitterionic nature of the stabilizer block and the weakly hydrophobic character of the core-forming block, no GPC eluent was found to be suitable for the non-crosslinked copolymers. DLS studies indicated that the z-average particle diameter remained essentially unchanged after amino acid functionalization (Tables S2, S3 and S4) while TEM analysis confirmed that such derivatization led to no change in the copolymer morphology (Figure 2c-d, Figure S2c-d, and Figure S3c-d).

Aqueous electrophoresis studies were conducted to obtain zeta potential vs. pH curves. For *cis*-diol functionalized linear PGEO5MA₂₆-PHPMA₁₇₀ spheres (Figure S7a), linear PGEO5MA₂₆-PHPMA₂₅₀ worms (Figure S8a) and crosslinked PGEO5MA₂₆-PHPMA₃₅₀-PEGDMA₂₀ vesicles (Figure 3a), and also the corresponding aldehyde-functionalized nano-objects obtained after periodate oxidation (Figure S7b, Figure S8b and Figure 3b), zeta potentials always remained close to zero over the whole pH range.

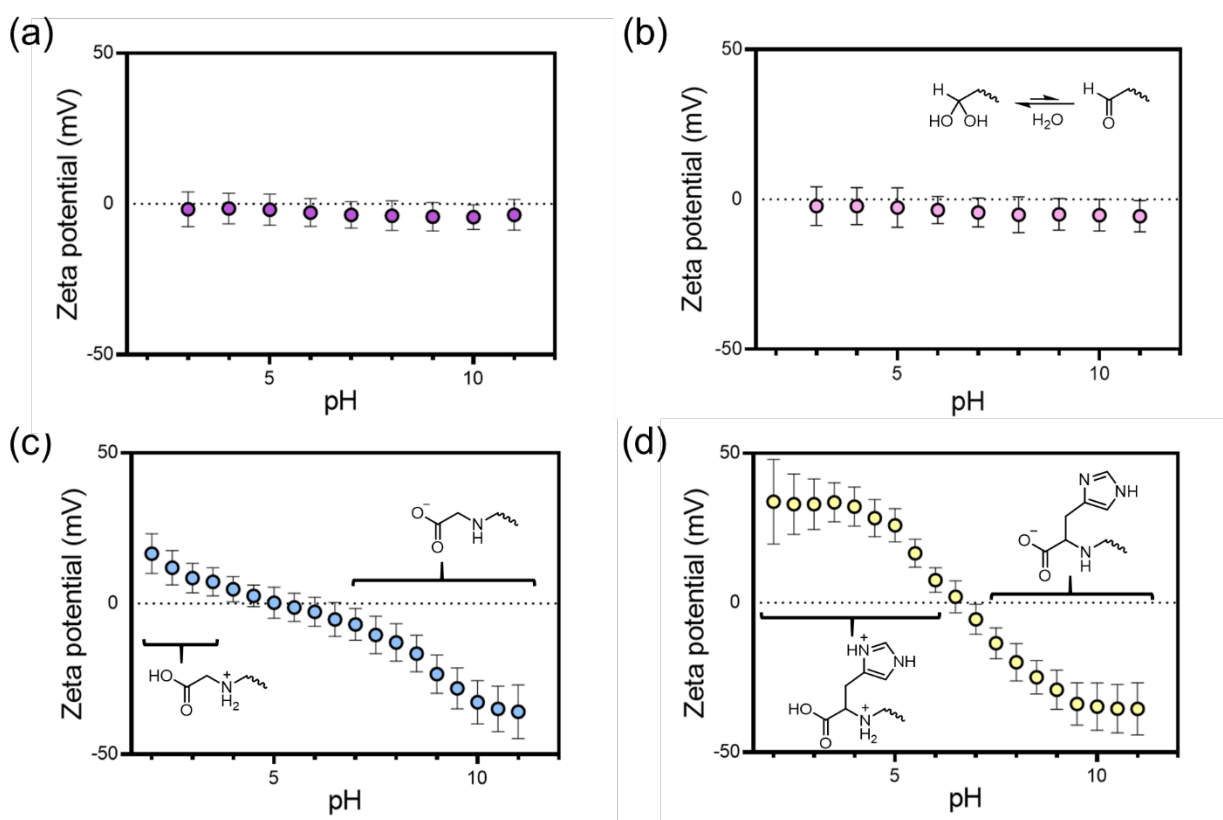


Figure 3. Zeta potential vs. pH plots obtained for (a) *cis*-diol-functionalized PGEO5MA₂₆-PHPMA₃₅₀-PEGDMA₂₀ vesicles, (b) aldehyde-functionalized PAGEO5MA₂₆-PHPMA₃₅₀-PEGDMA₂₀ vesicles, (c) glycine-functionalized PGlyGEO5MA₂₆-PHPMA₃₅₀-PEGDMA₂₀ vesicles and (d) histidine-functionalized PHisGEO5MA₂₆-PHPMA₃₅₀-PEGDMA₂₀ vesicles.

In contrast, glycine-functionalized nano-objects [e.g. PGlyGEO5MA₂₆-PHPMA₁₇₀ (Figure S7c), PGlyGEO5MA₂₆-PHPMA₂₅₀ (Figure S8c) and PGlyGEO5MA₂₆-PHPMA₃₅₀-PEGDMA₂₀ (Figure 3c)] exhibited positive zeta potentials between pH 3 and pH 4.5 owing to protonation of both the carboxylic acid and the secondary amine groups. An isoelectric point was observed at around pH 5, as expected for the zwitterionic form of the pendent amino acid. At higher pH, increasingly negative zeta potentials are obtained as the protonated secondary amine group is gradually converted into its neutral form.

Similarly, histidine-functionalized PHisGEO5MA₂₆-PHPMA₁₇₀ spheres (Figure S7d), PHisGEO5MA₂₆-PHPMA₂₅₀ worms (Figure S8d) and PHisGEO5MA₂₆-PHPMA₃₅₀-PEGDMA₂₀ vesicles (Figure 3d) each exhibited positive zeta potentials at low pH, indicating protonation of the pendent imidazole ring. An isoelectric point is observed at around pH 6.5 in each case. Above pH 6.5, zeta potentials became progressively more negative as the protonated secondary amine groups revert to their neutral form. These aqueous electrophoresis studies demonstrate how the electrophoretic footprint of such nano-objects can be tuned by amino acid functionalization.

The crosslinked PAGEO5MA₂₆-PHPMA₃₅₀-PEGDMA₂₀ vesicles were also reacted with a model globular protein, bovine serum albumin (BSA) via reductive amination using an excess of NaCNBH₃ as the reducing agent (Figures 4a and 4b). In this case the surface amine groups on the protein react with the pendent aldehyde groups located on the outer surface of the vesicles. The maximum number of BSA molecules adsorbed onto each vesicle was calculated using the approach reported by Balmer and co-workers.⁶⁴ The functionalized vesicles were then centrifuged and redispersed five times to ensure that any unbound BSA was removed from the aqueous dispersion. TEM analysis confirmed that the original vesicle morphology remained intact after exposure to BSA (Figure 4d). In order to determine whether the BSA had been successfully grafted onto the surface of the vesicles, aqueous electrophoresis studies were conducted (Figure 4c). The zeta potential vs. pH curve obtained for BSA alone indicated an isoelectric point (IEP) at pH 4.5, which is in good agreement with the literature.⁶⁵

In contrast, the aldehyde-functionalized vesicles exhibited approximately neutral character over the

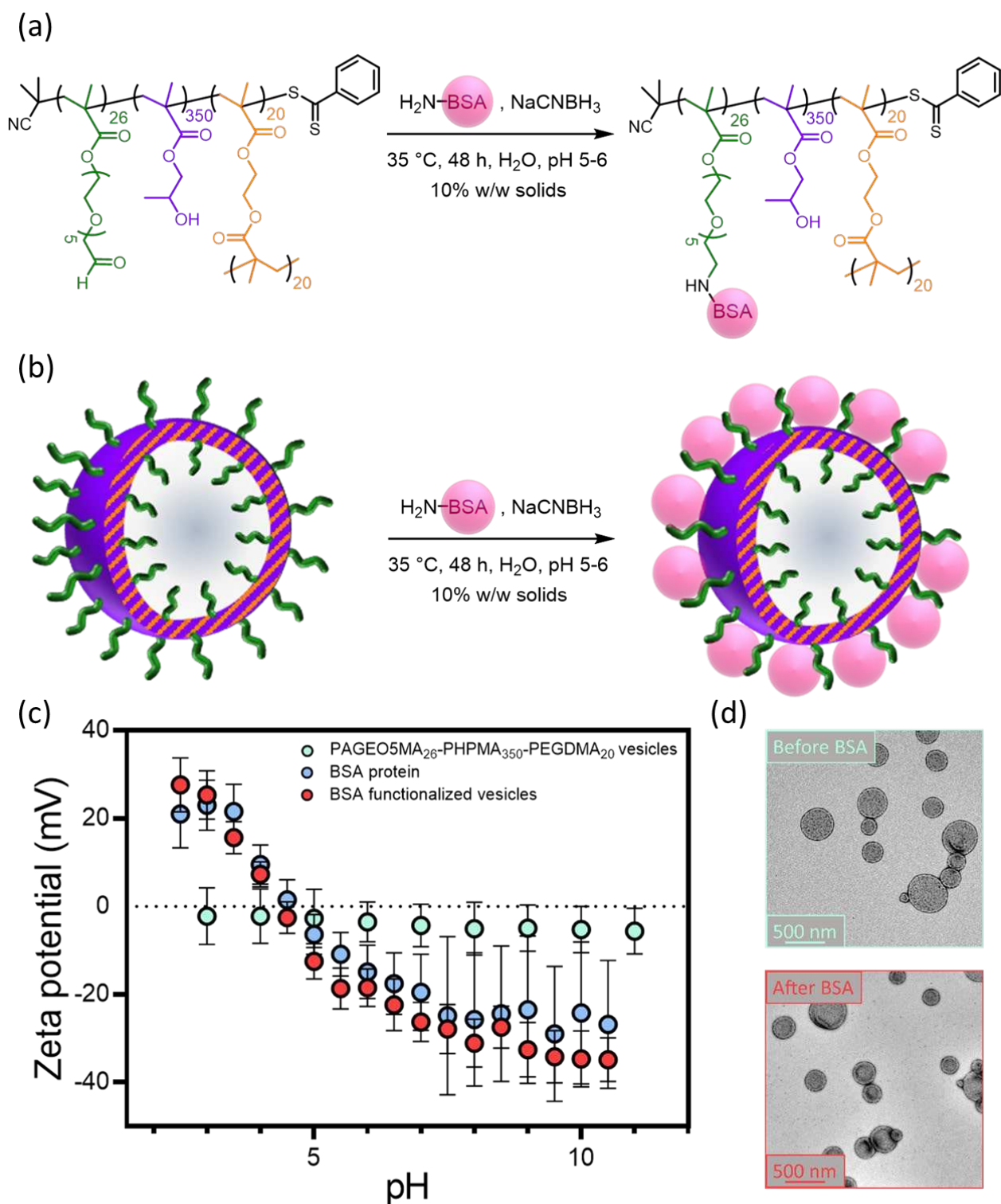


Figure 4. (a) Reductive amination of crosslinked PAGEO5MA₂₆-PPHMA₃₅₀-PEGDMA₂₀ vesicles with bovine serum albumin (BSA), (b) Schematic representation of the reaction of PAGEO5MA₂₆-PPHMA₃₅₀-PEGDMA₂₀ with BSA protein via reductive amination (N.B. vesicles and BSA protein are not shown to scale), (c) zeta potential vs. pH curves obtained for the original aldehyde-functionalized PAGEO5MA₂₆-PPHMA₃₅₀-PEGDMA₂₀ vesicles, BSA alone and the final BSA-functionalized PAGEO5MA₂₆-PPHMA₃₅₀-PEGDMA₂₀ vesicles and (d) TEM analysis confirmed that BSA functionalization did not affect the original vesicle morphology.

whole pH range. In principle, the BSA-grafted vesicles should exhibit a comparable electrophoretic footprint to that of the BSA alone. Indeed, a very similar zeta potential vs. pH curve was obtained, with essentially the same IEP being observed at around pH 4.5.

As a control experiment, the *cis*-diol-functionalized PGEO5MA₂₆-PHPMA₃₅₀-EGDMA₂₀ precursor vesicles were also exposed to BSA under the same conditions, followed by purification via five centrifugation-redispersion cycles (Figure S9). In this case, no change in the electrophoretic footprint was observed relative to the original vesicles (Figure S10). This confirms that surface aldehyde groups are required to ensure that the BSA molecules adsorb onto the vesicles.

Conclusions

We report the synthesis of a series of new diblock copolymer nano-objects *via* RAFT aqueous dispersion polymerization of HPMA using a new methacrylic monomer, GEO5MA, to prepare the water-soluble precursor block. The pendent *cis*-diol groups located within the PGEO5MA steric stabilizer chains can be selectively oxidized using aqueous sodium periodate to afford aldehyde-functional PAGEO5MA-HPMA nano-objects without loss of colloidal stability. In the case of PAGEO5MA-HPMA spheres or worms, periodate treatment does not affect the original copolymer morphology. In contrast, TEM studies indicate that periodate oxidation of the vesicles generates a minor population of worms. Fortunately, this unwanted partial loss of the original vesicular morphology can be prevented by introducing ethylene glycol dimethacrylate as a third block to crosslink the membrane-forming copolymer chains. Such covalently-stabilized PAGEO5MA-HPMA vesicles can be reacted with either an amino acid or a model globular protein (BSA) to form Schiff base linkages under mild conditions. In both cases, this leads to a significant change in the electrophoretic footprint of the vesicles. Such facile conjugation chemistry should offer potential bio-applications. For example, the BSA-functionalized vesicles should exhibit excellent stealth-like behavior in either *in vitro* or *in vivo* experiments.

Experimental

Materials

All reagents were used as received unless otherwise stated. GEO5MA monomer was synthesized by Dr C. P. Jesson at GEO Specialty Chemicals (Hythe, UK) as previously described.⁵⁹ 2-Hydroxypropyl methacrylate (HPMA, 97%) was kindly donated by GEO Specialty Chemicals (Hythe, UK). 4,4'-Azobis(4-cyanopentanoic acid) (ACVA; >98%), glycine ($\geq 98\%$), histidine ($\geq 98\%$), ethylene glycol dimethacrylate (EGDMA, 98%), sodium periodate (NaIO_4 , $\geq 99.8\%$), sodium cyanoborohydride (NaCNBH_3 , 95%), bovine serum albumin (BSA) and deuterium oxide (D_2O) were purchased from Sigma-Aldrich, UK. 2-Cyano-2-propyl dithiobenzoate (CPDB, >97%) was purchased from Strem Chemicals Ltd (Cambridge, UK). Ethanol, dichloromethane and diethyl ether were purchased from Fisher Scientific (UK). d_4 -Methanol and d_7 -dimethylformamide were purchased from Goss Scientific Instruments Ltd (Cheshire, UK). Deionized water was used for all experiments involving aqueous solutions.

Methods

^1H NMR spectroscopy. Spectra were recorded in either d_4 -methanol or d_7 -dimethylformamide using a 400 MHz Bruker Avance-400 spectrometer at 298 K with 16 scans being averaged per spectrum.

Aqueous electrophoresis. Zeta potentials for diblock copolymer nanoparticles were analyzed using a Malvern Zetasizer Nano ZS instrument equipped with a 4 mW He-Ne laser ($\lambda = 633 \text{ nm}$) operating at a fixed scattering angle of 173° . Samples were diluted to 0.1% w/w using 1 mM KCl, with either dilute NaOH or HCl being used for pH adjustment as required. Zeta potentials were calculated from the Henry equation using the Smoluchowski approximation.

Centrifugation. Centrifugation of BSA functionalized vesicles was conducted using a Thermo Heraeus Biofuge Pico centrifuge.

DMF Gel Permeation Chromatography (GPC). DMF GPC was used to determine the number-average molecular weights (M_n) and dispersities (\mathcal{D}) for all (co)polymers. The instrument set-up comprised two

Agilent PL gel 5 μm Mixed-C columns and a guard column connected in series to an Agilent 1260 Infinity GPC system operating at 60 °C. The GPC eluent was HPLC-grade DMF containing 10 mmol LiBr at a flow rate of 1.0 mL min⁻¹, the copolymer concentration was typically 1.0% w/w and calibration was achieved using a series of ten near-monodisperse poly(methyl methacrylate) standards ranging from 1 080 g mol⁻¹ to 905 000 g mol⁻¹. Chromatograms were analyzed using Agilent GPC/SEC software.

Dynamic Light Scattering (DLS). DLS studies were performed using a Malvern Zetasizer Nano-ZS instrument equipped with a 4 mW He-Ne laser ($\lambda = 633 \text{ nm}$) operating at a fixed scattering angle of 173°. Copolymer dispersions were diluted to 0.1% w/w using deionized water prior to light scattering studies at 25 °C, with 2 min being allowed for thermal equilibrium prior to each measurement. The hydrodynamic z-average particle diameter was calculated *via* the Stokes-Einstein equation.

Transmission Electron Microscopy (TEM). Copper/palladium TEM grids (Agar Scientific, UK) were coated in-house to yield a thin film of amorphous carbon and were subjected to a glow discharge for 30 s. Aqueous droplets of copolymer dispersions (5.0 μL , 0.1% w/w) were placed on freshly-treated grids for 1 min and then carefully blotted with filter paper to remove excess solution. An aqueous droplet of uranyl formate solution (5 μL , 0.75% w/w) was placed on each sample-loaded grid for 20 s and then blotted with filter paper to remove excess stain. This negative staining protocol was required to ensure sufficient electron contrast. Each grid was then carefully dried using a vacuum hose. Imaging was performed at 80 kV using an FEI Tecnai Spirit 2 microscope fitted with an Orius SC1000B camera.

Synthesis

Synthesis of the PGEO5MA₂₆ precursor by RAFT solution polymerization in ethanol

GEO5MA monomer (0.131 mol, 50.0 g), CPDB RAFT agent (3.98 mmol, 0.882 g), ACVA initiator (0.797 mmol, 0.223 g; CPDB/ACVA molar ratio = 5.0) and ethanol (34 g) were weighed into a 250 mL round-bottomed flask. The reaction mixture was degassed for 40 min using a N₂ purge before being placed into an oil bath set at 70 °C for 110 min. The polymerization was quenched by removing the flask from the oil bath and subsequent exposure of the reaction mixture to air. The GEO5MA

conversion was determined to be 58% by ^1H NMR spectroscopy. The crude PGEO5MA homopolymer was purified by precipitation into diethyl ether (to remove any unreacted monomer and other impurities), before being filtered and redissolved in methanol. This precipitation step was repeated and the purified homopolymer was dried in a vacuum oven set at 35 °C overnight to produce a pink/red viscous liquid. The mean DP of this PGEO5MA₂₆ precursor was determined by end-group analysis using ^1H NMR spectroscopy. The integrated signals between 7.34 and 8.03 ppm assigned to the five aromatic protons of the dithiobenzoate chain-end were compared to that of the five proton signals assigned to the methacrylate backbone at 0.78 – 2.71 ppm.

Synthesis of PGEO5MA₂₆-PHPMA_y diblock copolymer nanoparticles by RAFT aqueous dispersion polymerization of HPMA

The synthesis of PGEO5MA₂₆-PHPMA₁₇₀ spheres at 10% w/w solids is representative of the general protocol. HPMA monomer (2.77 mmol, 0.400 g), PGEO5MA₂₆ precursor (16.3 μmol , 0.165 g; target PHPMA DP = 170), ACVA initiator (4.08 μmol , 1.10 mg; PGEO5MA₂₆/ACVA molar ratio = 4.0) and water (5.10 g; targeting 10% w/w solids) were weighed into a 15 mL glass vial. The reaction mixture was purged using N₂ gas for 30 min and then the vial was placed in an oil bath set at 70 °C. After 4 h, the polymerization was quenched by removing the vial from the oil bath and exposing its contents to air. The final HPMA conversion was determined to be 99% by ^1H NMR spectroscopy by comparing the integrated vinyl HPMA monomer signals at 5.67 ppm and 6.16 ppm with that assigned to the methacrylate backbone signals at 0.81 - 2.30 ppm arising from the monomer and polymer.

Synthesis of PGEO5MA₂₆-PHPMA₃₅₀-PEGDMA₂₀ diblock copolymer nanoparticles by RAFT aqueous dispersion polymerization of HPMA

HPMA monomer (4.16 mmol, 0.600 g), PGEO5MA₂₆ precursor (11.9 μmol , 0.120 g; target PHPMA DP = 350), ACVA initiator (3.0 μmol , 0.80 mg; PGEO5MA₂₆/ACVA molar ratio = 4.0) and water (6.49 g; targeting 10% w/w solids) were weighed into a 15 mL glass vial. The reaction mixture was purged using N₂ gas for 30 min and then the vial was placed in an oil bath set at 70 °C. After 4 h, EGDMA crosslinker

(0.24 mmol, 0.047 g) and water (0.42 g) were added to the sample vial *via* syringe to maintain a copolymer concentration of 10% w/w. The reaction was left to proceed for 2 h at 70 °C before quenching by removing from the oil bath and exposure of the product to air. The final HPMA and EGDMA conversions were determined to be greater than 99% by ¹H NMR spectroscopy by comparing the integrated vinyl HPMA monomer and EGDMA signals at 5.67 ppm and 6.16 ppm with that assigned to the methacrylate backbone signals at 0.81 - 2.30 ppm arising from the monomer and polymer.

Oxidation and conjugation methods

Selective oxidation of PGEO5MA₂₆-PHPMA_y(-PEGDMA₂₀) diblock copolymer nanoparticles using sodium periodate

The general protocol for the oxidation of PGEO5MA₂₆-PHPMA₃₅₀-PEGDMA₂₀ vesicles in aqueous solution was as follows. Sodium periodate (64 μmol, 0.014 g) was dissolved in a 10% w/w aqueous dispersion of PGEO5MA₂₆-PHPMA₃₅₀-PEGDMA₂₀ vesicles (2.5 μmol, 1.50 g). A NaIO₄/*cis*-diol molar ratio of unity was used to target 100% oxidation of the PGEO5MA block. The reaction solution was stirred in the dark for 30 min at 22 °C. Degrees of oxidation were determined by ¹H NMR spectroscopy. The oxidation of PGEO5MA₂₆-PHPMA₁₇₀ spheres was also conducted at 10% w/w. For the more viscous aqueous dispersion of PGEO5MA₂₆-PHPMA₂₅₀ worms, the periodate oxidation was conducted at 5.0% w/w solids to ensure efficient stirring.

Amino acid conjugation to PAGEO5MA₂₆-PHPMA_y(-PEGDMA₂₀) diblock copolymer nanoparticles via reductive amination

The general protocol used for the reductive amination of PAGEO5MA₂₆-PHPMA_y(-PEGDMA₂₀) diblock copolymer nanoparticles with either glycine or histidine was as follows. A 10% w/w aqueous dispersion of PAGEO5MA₂₆-PHPMA₃₅₀-PEGDMA₂₀ vesicles (0.79 μmol, 1.00 g) was weighed into a 15 mL glass vial along with glycine (20 μmol, 1.5 mg; glycine/aldehyde molar ratio = 1.0). The reaction mixture was adjusted to pH 5-6 by adding either 0.1 M HCl or 0.1 M NaOH. Excess NaCNBH₃ (50 μmol, 3.2 mg; 2.45 mol excess) was carefully added to the reaction mixture, which was then stirred at 35 °C for 48 h to ensure maximum oxidation. The degree of oxidation was determined by ¹H NMR

spectroscopy to be more than 99% by comparing the integrated residual geminal diol signal at 6.09 ppm with the five methacrylate backbone protons and three methyl protons belonging to the PHPMA at 0.41-2.35 ppm. Essentially the same protocol was employed for histidine (22 μmol , 3.4 mg). The reductive amination of PGE05MA₂₆-PHPMA₃₅₀-PEGDMA₂₀ vesicles was also conducted at 10% w/w. For the relatively viscous aqueous dispersion of PGE05MA₂₆-PHPMA₂₅₀ worms, the reductive amination was conducted at 5.0% w/w solids to ensure efficient stirring.

Functionalization of PGE05MA₂₆-PHPMA₃₅₀-PEGDMA₂₀ diblock copolymer vesicles with bovine serum albumin (BSA) via reductive amination

A 10% w/w copolymer dispersion of crosslinked PGE05MA₂₆-PHPMA₃₅₀-PEGDMA₂₀ vesicles (26.6 μmol , 1.0 g) was weighed into a 15 mL glass vial along with BSA (0.13 μmol , 8.80 mg; BSA/aldehyde molar ratio = 0.0019). The solution pH was adjusted to pH 5-6 by addition of either 0.1 M HCl or 0.1 M NaOH. NaCNBH₃ (0.33 μmol , 0.20 mg; 2.45 mol excess) was added to the reaction mixture, which was then stirred at 35 °C for 48 h. The copolymer dispersion was centrifuged at 15,000 rpm for 12 min and then redispersed in deionized water to remove excess BSA remaining in the aqueous phase. This protocol was repeated four times to ensure that all non-adsorbed BSA was removed from the aqueous dispersion.

Acknowledgements

We thank the EPSRC for a CDT PhD studentship for E.E.B. (EP/L016281) and GEO Specialty Chemicals for additional financial support of this project and also for permission to publish these results. S.P.A. acknowledges an EPSRC *Established Career* Particle Technology Fellowship grant (EP/R003009).

References

- 1 S. Newman, Note on colloidal dispersions from block copolymers, *Journal of Applied Polymer Science*, 1962, **6**, S15–S16.
- 2 G. M. Burnett, P. Mears and C. Paton, Downloaded by The University of Manchester Library on 11/30, *Trans. Faraday Society*, 1962, **58**, 737–746.
- 3 S. Krause, Dilute solution properties of a styrene-methyl methacrylate block copolymer, *Journal of Physical Chemistry*, 1964, **68**, 1948–1955.
- 4 Z. Gao, S. K. Varshney, S. Wong and A. Eisenberg, Block Copolymer “Crew-Cut” Micelles in Water, *Macromolecules*, 1994, **27**, 7923–7927.
- 5 L. Zhang and A. Eisenberg, Multiple Morphologies of “Crew-Cut” Aggregates of Polystyrene-*b*-poly(acrylic acid) Block Copolymers, *Science*, 1995, **268**, 1728–1731.
- 6 S. L. Canning, G. N. Smith and S. P. Armes, A Critical Appraisal of RAFT-Mediated Polymerization-Induced Self-Assembly, *Macromolecules*, 2016, **49**, 1985–2001.
- 7 B. Charleux, G. Delaittre, J. Rieger and F. D’agosto, Polymerization-Induced Self-Assembly: From Soluble Macromolecules to Block Copolymer Nano-Objects in One Step, *Macromolecules*, 2012, **45**, 6753–6765.
- 8 F. D’Agosto, J. Rieger, M. Lansalot, D. F, R. J and L. M, RAFT-Mediated Polymerization-Induced Self-Assembly, *Angewandte Chemie - International Edition*, 2019, **59**, 2–27.
- 9 A. Blanazs, A. J. Ryan and S. P. Armes, Predictive Phase Diagrams for RAFT Aqueous Dispersion Polymerization: Effect of Block Copolymer Composition, Molecular Weight, and Copolymer Concentration, *Macromolecules*, 2012, **45**, 5099–5107.
- 10 L. D. Blackman, K. E. B. Doncom, M. I. Gibson and R. K. O’Reilly, Comparison of photo- and thermally initiated polymerization-induced self-assembly: a lack of end group fidelity drives the formation of higher order morphologies, *Polymer Chemistry*, 2017, **8**, 2860–2871.
- 11 E. R. Jones, M. Semsarilar, P. Wyman, M. Boerakker and S. P. Armes, Addition of water to an alcoholic RAFT PISA formulation leads to faster kinetics but limits the evolution of copolymer morphology, *Polymer Chemistry*, 2016, **7**, 851–859.
- 12 J. Chiefari, Y. K. Chong, F. Ercole, J. Krstina, J. Jeffery, T. P. T Le, R. T. A Mayadunne, G. F. Meijs, C. L. Moad, G. Moad, E. Rizzardo and S. H. Thang, Living Free-Radical Polymerization by Reversible Addition-Fragmentation Chain Transfer: The RAFT Process, *Macromolecules*, 1998, **31**, 5559–5562.
- 13 D. J. Keddie, G. Moad, E. Rizzardo and S. H. Thang, RAFT agent design and synthesis, *Macromolecules*, 2012, **45**, 5321–5342.
- 14 Y. Du, S. Jia, Y. Chen, L. Zhang and J. Tan, Type I Photoinitiator-Functionalized Block Copolymer Nanoparticles Prepared by RAFT-Mediated Polymerization-Induced Self-Assembly, *ACS Macro Letters*, 2021, **10**, 297–306.
- 15 J. Rosselgong, A. Blanazs, P. Chambon, M. Williams, M. Semsarilar, J. Madsen, G. Battaglia and S. P. Armes, Thiol-Functionalized Block Copolymer Vesicles, *ACS Macro Letters*, 2012, **1**, 1041–1045.

- 16 K. A. Simon, N. J. Warren, B. Mosadegh, M. R. Mohammady, G. M. Whitesides and S. P. Armes, Disulfide-Based Diblock Copolymer Worm Gels: A Wholly-Synthetic Thermoreversible 3D Matrix for Sheet-Based Cultures, *Biomacromolecules*, 2015, **16**, 3952–3958.
- 17 F. L. Hatton, J. R. Lovett and S. P. Armes, Synthesis of well-defined epoxy-functional spherical nanoparticles by RAFT aqueous emulsion polymerization, *Polymer Chemistry*, 2017, **8**, 4856–4868.
- 18 F. L. Hatton, A. M. Park, Y. Zhang, G. D. Fuchs, C. K. Ober and S. P. Armes, Aqueous one-pot synthesis of epoxy-functional diblock copolymer worms from a single monomer: new anisotropic scaffolds for potential charge storage applications, *Polymer Chemistry*, 2019, **10**, 194–200.
- 19 F. L. Hatton, M. J. Derry and S. P. Armes, Rational synthesis of epoxy-functional spheres, worms and vesicles by RAFT aqueous emulsion polymerisation of glycidyl methacrylate, *Polymer Chemistry*, 2020, **11**, 6343–6355.
- 20 P. Chambon, A. Blanazs, G. Battaglia and S. P. Armes, Facile Synthesis of Methacrylic ABC Triblock Copolymer Vesicles by RAFT Aqueous Dispersion Polymerization, *Macromolecules*, 2012, **45**, 5081–5090.
- 21 X. Dai, L. Yu, Y. Zhang, L. Zhang and J. Tan, Polymerization-Induced Self-Assembly via RAFT-Mediated Emulsion Polymerization of Methacrylic Monomers, *Macromolecules*, 2019, **52**, 7468–7476.
- 22 Z. Cui, H. Cao, Y. Ding, P. Gao, X. Lu and Y. Cai, Compartmentalization of an ABC triblock copolymer single-chain nanoparticle: via coordination-driven orthogonal self-assembly, *Polymer Chemistry*, 2017, **8**, 3755–3763.
- 23 S. J. Byard, M. Williams, B. E. McKenzie, A. Blanazs and S. P. Armes, Preparation and Cross-Linking of All-Acrylamide Diblock Copolymer Nano-Objects via Polymerization-Induced Self-Assembly in Aqueous Solution, *Macromolecules*, 2017, **50**, 1482–1493.
- 24 F. H. Sobotta, F. Hausig, D. O. Harz, S. Hoeppener, U. S. Schubert and J. C. Brendel, Oxidation-responsive micelles by a one-pot polymerization-induced self-assembly approach, *Polymer Chemistry*, 2018, **9**, 1593–1602.
- 25 G. Mellot, J.-M. Guigner, L. Bouteiller, F. Stoffelbach and J. Rieger, Templated PISA: Driving Polymerization-Induced Self-Assembly towards Fibre Morphology, *Angewandte Chemie International Edition*, 2019, **58**, 3173–3177.
- 26 J. R. Lovett, N. J. Warren, S. P. Armes, M. J. Smallridge and R. B. Cracknell, Order-Order Morphological Transitions for Dual Stimulus Responsive Diblock Copolymer Vesicles, *Macromolecules*, 2016, **49**, 1016–1025.
- 27 J. R. Lovett, N. J. Warren, L. P. D. Ratcliffe, M. K. Kocik and S. P. Armes, pH-responsive non-ionic diblock copolymers: Ionization of carboxylic acid end-groups induces an order-order morphological transition, *Angewandte Chemie - International Edition*, 2015, **54**, 1279–1283.
- 28 V. J. Cunningham, A. M. Alswieleh, K. L. Thompson, M. Williams, G. J. Leggett, S. P. Armes and O. M. Musa, Poly(glycerol monomethacrylate)-poly(benzyl methacrylate) diblock copolymer nanoparticles via RAFT emulsion polymerization: Synthesis, characterization, and interfacial activity, *Macromolecules*, 2014, **47**, 5613–5623.

- 29 R. Deng, M. J. Derry, C. J. Mable, Y. Ning and S. P. Armes, Using Dynamic Covalent Chemistry to Drive Morphological Transitions: Controlled Release of Encapsulated Nanoparticles from Block Copolymer Vesicles, *Journal of the American Chemical Society*, 2017, **139**, 7616–7623.
- 30 R. Deng, Y. Ning, E. R. Jones, V. J. Cunningham, N. J. W. Penfold and S. P. Armes, Stimulus-responsive block copolymer nano-objects and hydrogels via dynamic covalent chemistry, *Polymer Chemistry*, 2017, 5374–5380.
- 31 I. Canton, N. J. Warren, A. Chahal, K. Amps, A. Wood, R. Weightman, E. Wang, H. Moore and S. P. Armes, Mucin-inspired thermoresponsive synthetic hydrogels induce stasis in human pluripotent stem cells and human embryos, *ACS Central Science*, 2016, **2**, 65–74.
- 32 M. B. Smith and J. March, *March's advanced organic chemistry: reactions, mechanisms, and structure*, John Wiley & Sons, Inc., Hoboken, NJ, 2007.
- 33 J. Collins, K. Kempe, P. Wilson, C. A. Blindauer, M. P. McIntosh, T. P. Davis, M. R. Whittaker and D. M. Haddleton, Stability Enhancing N-Terminal PEGylation of Oxytocin Exploiting Different Polymer Architectures and Conjugation Approaches, *Biomacromolecules*, 2016, **17**, 2755–2766.
- 34 J. Collins, S. J. Wallis, A. Simula, M. R. Whittaker, M. P. McIntosh, P. Wilson, T. P. Davis, D. M. Haddleton and K. Kempe, Comb Poly(Oligo(2-Ethyl-2-Oxazoline)Methacrylate)-Peptide Conjugates Prepared by Aqueous Cu(0)-Mediated Polymerization and Reductive Amination, *Macromolecular Rapid Communications*, 2017, **38**, 1600534.
- 35 C. Scholz, M. Iijima, Y. Nagasaki and K. Kataoka, *Macromolecules*, 1995, **28**, 7295–7297.
- 36 Y. Nagasaki, T. Okada, C. Scholz, M. Iijima, M. Kato and K. Kataoka, The reactive polymeric micelle based on an aldehyde-ended poly(ethylene glycol)/poly(lactide) block copolymer, *Macromolecules*, 1998, **31**, 1473–1479.
- 37 M. Iijima, Y. Nagasaki, T. Okada, M. Kato and K. Kataoka, Core-Polymerized Reactive Micelles from Heterotelechelic Amphiphilic Block Copolymers, *Macromolecules*, 1999, **32**, 1140–1146.
- 38 H. Otsuka, Y. Nagasaki and K. Kataoka, Surface characterization of functionalized polylactide through the coating with heterobifunctional poly(ethylene glycol)/ polylactide block copolymers, *Biomacromolecules*, 2000, **1**, 39–48.
- 39 R. J. Mancini, J. Lee and H. D. Maynard, Trehalose glycopolymers for stabilization of protein conjugates to environmental stressors, *Journal of the American Chemical Society*, 2012, **134**, 8474–8479.
- 40 B. Karagoz, L. Esser, H. T. Duong, J. S. Basuki, C. Boyer and T. P. Davis, Polymerization-Induced Self-Assembly (PISA) – control over the morphology of nanoparticles for drug delivery applications, *Polymer Chemistry*, 2014, **5**, 350–355.
- 41 J. Liu, H. Duong, M. R. Whittaker, T. P. Davis and C. Boyer, Synthesis of Functional Core, Star Polymers via RAFT Polymerization for Drug Delivery Applications, *Macromolecular Rapid Communications*, 2012, **33**, 760–766.
- 42 L. Qiu, C. R. Xu, F. Zhong, C. Y. Hong and C. Y. Pan, Fabrication of Functional Nano-objects through RAFT Dispersion Polymerization and Influences of Morphology on Drug Delivery, *ACS Applied Materials and Interfaces*, 2016, **8**, 18347–18359.

- 43 L. Qiu, C. R. Xu, F. Zhong, C. Y. Hong and C. Y. Pan, Cross-Linked Nano-Objects Containing Aldehyde Groups: Synthesis via RAFT Dispersion Polymerization and Application, *Macromolecular Chemistry and Physics*, 2016, **217**, 1047–1056.
- 44 A. W. Jackson and D. A. Fulton, Triggering polymeric nanoparticle disassembly through the simultaneous application of two different stimuli, *Macromolecules*, 2012, **45**, 2699–2708.
- 45 G. Sun, H. Fang, C. Cheng, P. Lu, K. Zang, A. V. Walker, J.-S. A. Taylor and K. L. Wooley, Benzaldehyde-functionalised polymer vesicles, *ACS Nano*, 2009, **3**, 673–681.
- 46 G. S. Heo, S. Cho and K. L. Wooley, Aldehyde-functional polycarbonates as reactive platforms, *Polymer Chemistry*, 2014, **5**, 3555–3558.
- 47 G. Sun, C. Cheng and K. L. Wooley, Reversible Addition Fragmentation Chain Transfer Polymerization of 4-Vinylbenzaldehyde, *Macromolecules*, 2007, **40**, 793–795.
- 48 S. N. S. S. Alconcel, S. H. Kim, L. Tao and H. D. Maynard, Synthesis of biotinylated aldehyde polymers for biomolecule conjugation, *Macromolecular Rapid Communications*, 2013, **34**, 983–989.
- 49 J. Hwang, R. C. Li and H. D. Maynard, Well-defined polymers with activated ester and protected aldehyde side chains for bio-functionalization, *Journal of Controlled Release*, 2007, **122**, 279–286.
- 50 C. L. I. Ronald, R. M. Broyer and H. D. Maynard, in *Journal of Polymer Science, Part A: Polymer Chemistry*, John Wiley & Sons, Ltd, 2006, vol. 44, pp. 5004–5013.
- 51 T. Bilgic and H. A. Klok, Oligonucleotide Immobilization and Hybridization on Aldehyde-Functionalized Poly(2-hydroxyethyl methacrylate) Brushes, *Biomacromolecules*, 2015, **16**, 3657–3665.
- 52 M. A. Gauthier and A. Klok, Arginine-Specific Modification of Proteins with Polyethylene Glycol, *Biomacromolecules*, 2011, **12**, 482–493.
- 53 J. Wang, P. Karami, N. C. Ataman, D. P. Pioletti, T. W. J. Steele and H. A. Klok, Light-Activated, Bioadhesive, Poly(2-hydroxyethyl methacrylate) Brush Coatings, *Biomacromolecules*, 2020, **21**, 240–249.
- 54 M. A. Gauthier, M. Ayer, J. Kowal, F. R. Wurm and H.-A. Klok, Arginine-specific protein modification using α -oxo-aldehyde functional polymers prepared by atom transfer radical polymerization, *Polymer Chemistry*, 2011, **2**, 1490–1498.
- 55 L. Tao, G. Mantovani, F. Lecolley and D. M. Haddleton, α -aldehyde terminally functional methacrylic polymers from living radical polymerization: Application in protein conjugation “ pegylation,” *Journal of the American Chemical Society*, 2004, **126**, 13220–13221.
- 56 B. S. Murray and D. A. Fulton, Dynamic covalent single-chain polymer nanoparticles, *Macromolecules*, 2011, **44**, 7242–7252.
- 57 D. E. Whitaker, C. S. Mahon and D. A. Fulton, Thermoresponsive Dynamic Covalent Single-Chain Polymer Nanoparticles Reversibly Transform into a Hydrogel, *Angewandte Chemie International Edition*, 2013, **52**, 956–959.

- 58 B. S. Murray, A. W. Jackson, C. S. Mahon and D. A. Fulton, Reactive thermoresponsive copolymer scaffolds, *Chemical Communications*, 2010, **46**, 8651–8653.
- 59 E. E. Brotherton, C. P. Jesson, N. J. Warren, M. J. Smallridge and S. P. Armes, New Aldehyde-Functional Methacrylic Water-Soluble Polymers, *Angewandte Chemie International Edition*, 2021, **60**, 12032–12037.
- 60 Y. Li and S. P. Armes, RAFT Synthesis of Sterically Stabilized Methacrylic Nanolatexes and Vesicles by Aqueous Dispersion Polymerization, *Angewandte Chemie*, 2010, **122**, 4136–4140.
- 61 I. Bannister, N. C. Billingham, S. P. Armes, S. P. Rannard and P. Findlay, Development of Branching in Living Radical Copolymerization of Vinyl and Divinyl Monomers, *Macromolecules*, 2006, **39**, 7483–7492.
- 62 A. Blanazs, J. Madsen, G. Battaglia, A. J. Ryan and S. P. Armes, Mechanistic insights for block copolymer morphologies: How do worms form vesicles?, *Journal of the American Chemical Society*, 2011, **133**, 16581–16587.
- 63 P. Chambon, A. Blanazs, G. Battaglia and S. P. Armes, Facile synthesis of methacrylic ABC triblock copolymer vesicles by RAFT aqueous dispersion polymerization, *Macromolecules*, 2012, **45**, 5081–5090.
- 64 J. A. Balmer, S. P. Armes, P. W. Fowler, T. Tarnai, Z. Gáspár, K. A. Murray and N. S. J. Williams, Packing efficiency of small silica particles on large latex particles: A facile route to colloidal nanocomposites, *Langmuir*, 2009, **25**, 5339–5347.
- 65 K. M. Au and S. P. Armes, Heterocoagulation as a facile route to prepare stable serum albumin-nanoparticle conjugates for biomedical applications: Synthetic protocols and mechanistic insights, *ACS Nano*, 2012, **6**, 8261–8279.